inorganics

MDPI

Article

Synthesis of $LiAlH_4$ Nanoparticles Leading to a Single Hydrogen Release Step upon Ti Coating

Lei Wang and Kondo-Francois Aguey-Zinsou *

Merlin group, School of Chemical Engineering, The University of New South Wales, Sydney 2052, Australia; lei.wang@unsw.edu.au

* Correspondence: f.aguey@unsw.edu.au; Tel.: +61-293-857-970

Academic Editor: Torben R. Jensen

Received: 20 May 2017; Accepted: 3 June 2017; Published: 7 June 2017

Abstract: Lithium aluminum hydride ($LiAlH_4$) is an interesting high capacity hydrogen storage material with fast hydrogen release kinetics when mechanically activated with additives. Herein, we report on a novel approach to produce nanoscale $LiAlH_4$ via a bottom-up synthesis. Upon further coating of these nanoparticles with Ti, the composite nanomaterial was found to decompose at 120 °C in one single and extremely sharp exothermic event with instant hydrogen release. This finding implies a significant thermodynamic alteration of the hydrogen properties of $LiAlH_4$ induced by the synergetic effects of the Ti catalytic coating and nanosizing effects. Ultimately, the decomposition path of $LiAlH_4$ was changed to $LiAlH_4 \rightarrow Al + LiH + 3/2H_2$.

Keywords: alanate; lithium aluminum hydride; nanosizing; core–shell; hydrogen storage

1. Introduction

Hydrogen holds enormous potential to be the ultimate energy carrier of the future [1–5]. Yet the lack of an effective method for storing hydrogen with high density currently restrains its widespread utilization. Solid state hydride materials offer promising possibilities to deliver high capacity, safe, and compact hydrogen storage systems [5,6]. However, so far no material satisfies all the requirements for practical mobile application [3]. For hydrogen storage purposes, $LiAlH_4$ is one of the most promising and interesting candidates owing to its competitive total hydrogen capacity as well as its low temperature for hydrogen release with fast kinetics [3,6]. When doped with catalysts, about 75% of its stored hydrogen can be released below 100 °C in about 1.5 h, while 30 min is required when at 150 °C [7–11]. A particularity of $LiAlH_4$ is the exothermic nature of its initial hydrogen release following the widely accepted Steps 1–3 [12–14].

Step 1a	150–175 °C	
$LiAlH_{4(solid)} \rightarrow LiAlH_{4(liquid)}$	endothermic	
Step 1b	150–200 °C	
$LiAlH_{4(liquid)} \rightarrow 1/3\ Li_3AlH_{6(solid)} + 2/3\ Al + H_2\uparrow$	exothermic	5.3 mass % H_2
Step 2	200–270 °C	
$Li_3AlH_{6(solid)} \rightarrow 3\ LiH + Al + 3/2\ H_2\uparrow$	endothermic	2.6 mass % H_2
Step 3	400–440 °C	
$LiH + Al \rightarrow LiAl + 1/2\ H_2\uparrow$	endothermic	2.6 mass % H_2

Step 1a corresponds to the melting of $LiAlH_4$ quickly followed by the exothermic Step 1b with a reported ΔH of decomposition of -10 kJ·mol^{-1} H_2 [1,2]. Hence, the reversibility of this step is generally believed to be thermodynamically impossible under practical conditions of temperature and pressure [3,4]. Indeed, theoretical studies have suggested the need for extreme hydrogen pressures

>100 MPa at room temperature for the direct regeneration of $LiAlH_4$ from Li_3AlH_6 [2,3,5]. In Step 2, Li_3AlH_6 decomposes via an endothermic reaction with a ΔH of 25 kJ·mol^{-1} H_2 [6]. Hence the regeneration of Li_3AlH_6 from LiH and Al can be considered thermodynamically feasible. The last decomposition occurring at temperatures higher than 400 °C precludes this step from practical hydrogen storage application, reducing the total hydrogen capacity to 7.9 mass % H_2 (below 300 °C).

Accordingly, current investigations have mainly focused at the destabilization of $LiAlH_4$ via catalyst doping and/or mechanical milling with additives to further improve its dehydrogenation kinetics and potentially achieve some degree of reversibility. Hence, upon mechanically milling $LiAlH_4$ with $TiCl_3$, $ZrCl_4$, or nanosized Ni, lower hydrogen desorption temperatures have been achieved [7–11]; however, with no successful rehydrogenation. Indirect rehydrogenation routes have also been demonstrated through the use of wet synthesis approaches involving the formation of solvent adducts of $LiAlH_4$—i.e., THF, Et_2O, diglyme, and Me_2O—and in most cases activated/catalyzed Al [12–16]. Such an indirect route not only needs to be performed off-board while requiring the additional process of desolvation, but also can compromise the integrity of activated doped $LiAlH_4$. For example, for the multi-step regeneration method developed by Graetz et al., and involving the use of THF, successive doping and redoping is required to maintain the same hydrogen storage performance before and after each desolvation of THF [13]. Chen et al. achieved a partial direct reversibility of titanium-catalyzed Li_3AlH_6, i.e., to reverse Step 2, without the need of solvent desolvation under a hydrogen pressure of 40 MPa only [17]. However, the evidence of regenerated Li_3AlH_6 was a few non-exclusive XRD peaks without structure determination of the rehydrided Li_3AlH_6 and despite this promising result no follow-up study was reported.

Previous work from our group revealed the possibility of direct rehydrogenation of $LiAlH_4$ via nanoconfinement in mesoporous carbon and this could be achieved under mild conditions of pressures and temperatures following the assumed route of $3LiH + Al + 3/2H_2 \rightarrow Li_3AlH_6 + 2Al + 3H_2 \rightarrow 3LiAlH_4$ [18]. Furthermore, positive alternations of hydrogen storage properties were observed with a core–shell method for the individual stabilization of $NaBH_4$ or LiH nanoparticles avoiding some drawbacks of porous host scaffolds [19,20]. This impetus led to the current work which investigated a simple route for the synthesis of isolated $LiAlH_4$ nanoparticles and their stabilization for hydrogen cycling through a core–shell approach, with Ti acting as a shell facilitating the retention of molten $LiAlH_4$ upon dehydrogenation as well as a "gateway" for hydrogen absorption/desorption. Ti based additives have been widely studied via top–down ball milling for $LiAlH_4$, as well as with other alanate systems e.g., $NaAlH_4$ and $Mg(AlH_4)_2$ with promising results, i.e., much improved hydrogen storage properties [21–26]. Indeed, Kojima et al. determined the catalytic effects of various metal chlorides on $LiAlH_4$, and revealed their positive effects in terms of hydrogen release in the order of $TiCl_3 > ZrCl_4 > VCl_3 > NiCl_2 > ZnCl_2$ [27]. Amama et al. also investigated the properties of ball milled $LiAlH_4$ with various dopants, and concluded that Ti-based additives lead to the most enhancement in terms of dehydrogenation kinetics and reduction of the decomposition temperature [9]. Based on these previous findings and the potential of a nanosizied approach [28,29], it is thus interesting to investigate the effect of Ti doping/coating on nanosized $LiAlH_4$.

2. Results

In principle, the nanosynthesis of $LiAlH_4$ can be achieved via common solvent evaporation methods [30]. In this procedure, a solution of the nanoparticles' precursor is evaporated under high vacuum [31,32] and this results in the rapid nucleation of the solute materials because of the supersaturated nature of the solution. The growth of the nuclei is then limited via steric repulsion of suitable stabilizers. Currently, the syntheses of most nanoparticles through solvent evaporation are performed in an aqueous solution [33,34]. However, for hydride materials which are highly oxidized by water, the synthesis should be performed under non-aqueous environments. To achieve the preparation of nanosized $LiAlH_4$ particles, we thus used a THF solution of 2M $LiAlH_4$ with 1-dodecanethiol as a stabilizer and weak capping ligand.

As shown in Figure 1, at the end of the evaporation process the XRD pattern of the material confirmed the preparation of $LiAlH_4$ with broader diffraction peaks indicating its nanostructure. The nanosized nature of the material was confirmed by TEM analysis showing isolated spherical nanoparticles with a particle size ranging from 2 to 16 nm (Figure 2).

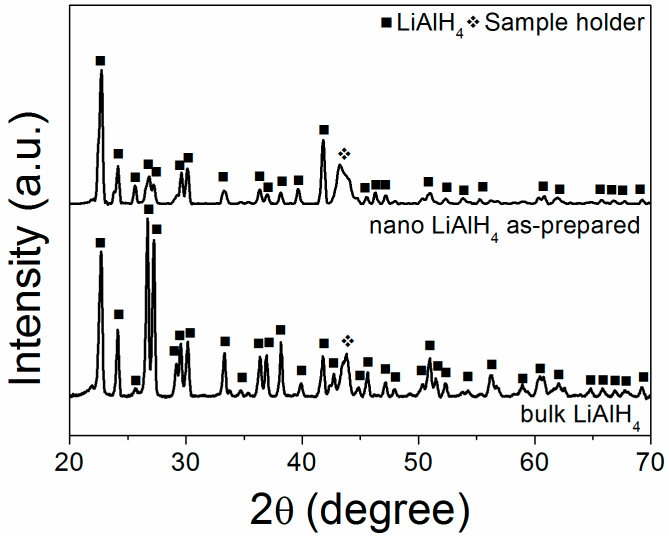

Figure 1. XRD of as-prepared nanosized $LiAlH_4$ via solvent evaporation and commercial bulk $LiAlH_4$.

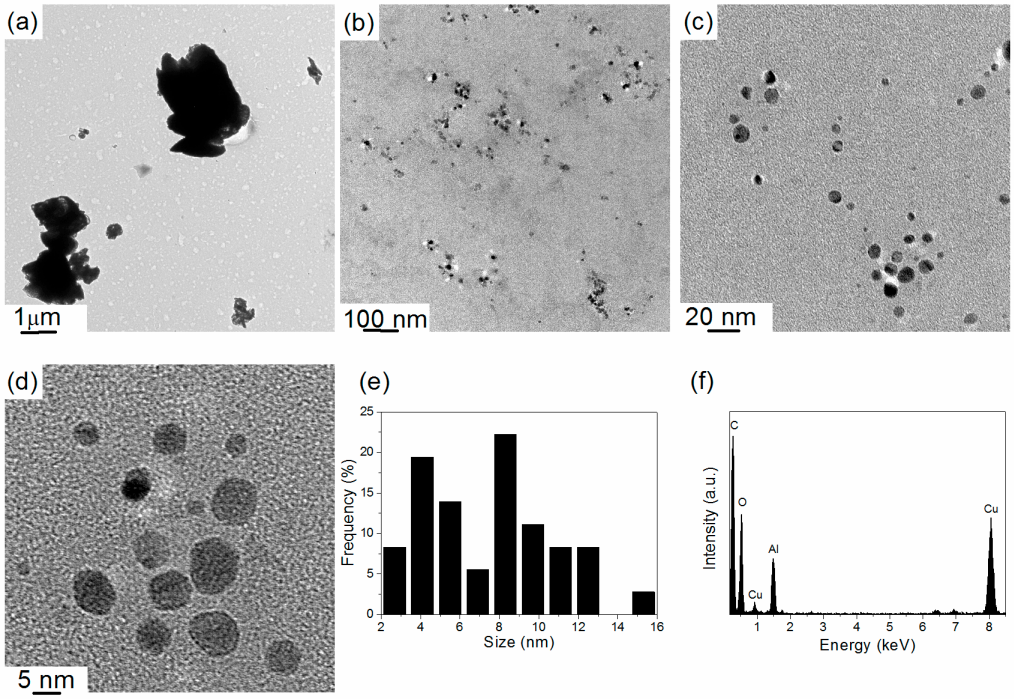

Figure 2. TEM images of (**a**) commercial bulk $LiAlH_4$ and (**b**–**d**) as-prepared nanosized $LiAlH_4$ via solvent evaporation; (**e**) corresponding particle size distribution and (**f**) EDS spectrum.

EDS analysis further confirmed the Al content of these nanoparticles that were thus believed to correspond to $LiAlH_4$ (Figure 2f). In comparison, bulk $LiAlH_4$ was imaged as large particles with no defined morphology (Figure 2a), hence the synthesis of nanosized $LiAlH_4$ was successful.

The hydrogen desorption properties of these nanoparticles were determined by TGA/DSC/MS. As shown in Figure 3, the as-prepared $LiAlH_4$ nanoparticles desorbed hydrogen in a similar way to

bulk $LiAlH_4$ with the release of hydrogen occurring in two steps before 300 °C. The small additional exothermic peak at 145 °C was assigned to the reaction of the thiol head of the surfactant with $LiAlH_4$ at the surface of the nanoparticles. The similarities of the decompositions behavior is inherent to the inability of the surfactant to contain the melted $LiAlH_4$ and thus a loss of the nanosize feature in the favor of larger molten agglomerates behaving like bulk $LiAlH_4$. The decomposition of the dodecanthiol as evidenced by mass spectrometry near 220 °C [35] further supports this hypothesis (Figure 3d).

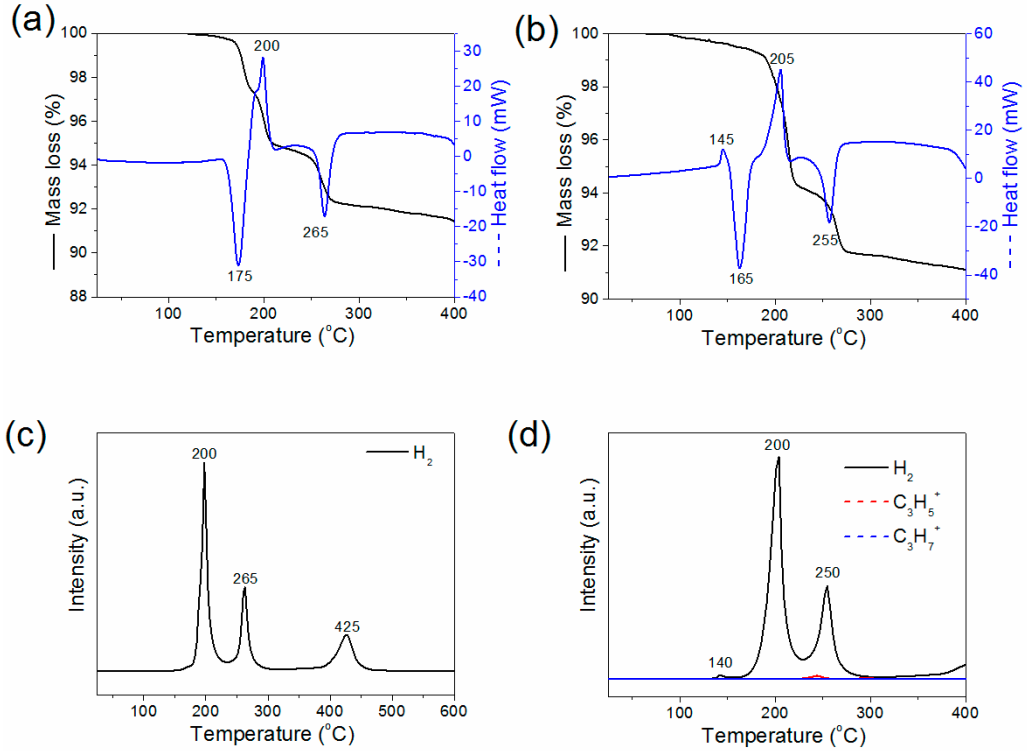

Figure 3. TGA/DSC for (**a**) commercial bulk $LiAlH_4$; (**b**) as-prepared nanosized $LiAlH_4$ via solvent evaporation, and (**c**,**d**) respective hydrogen desorption profile as followed by mass spectrometry. The fragments $C_3H_5^+$ and $C_3H_7^+$ correspond to the decomposition of the 1-dodecanethiol surfactant [36]. The decreasing heat flow peaks correspond to an endothermic process.

In order to better stabilize these nanoparticles and contain the melt, we aimed at a core–shell strategy [20]. whereby the core $LiAlH_4$ is contained within a metallic shell. To this aim, Ti was thought to be the best option because it is a well-known catalyst for other alanate systems including $NaAlH_4$ and $Mg(AlH_4)_2$ [21,26,37]. In particular, Ti-based additives have shown benefit for enhancing dehydrogenation kinetics and reduction of the decomposition temperature of alanates [9]. Ti also forms a hydride and has good hydrogen diffusion properties [38,39]. In addition, $TiCl_3$ can be readily reduced by $LiAlH_4$, and thus could form through the transmetalation method [19,20,31]. A core–shell structure assuming that the reduction rate of the titanium precursor at the surface of the $LiAlH_4$ nanoparticles can be controlled to form a continuous shell [40].

To coat the nanosized $LiAlH_4$ particles with Ti, $LiAlH_4$ nanoparticles were suspended in pentane where they are insoluble and a solution of $TiCl_3$ in pentane was added dropwise. In this process, $TiCl_3$ is reduced at the surface of $LiAlH_4$ nanoparticles following reaction (1).

$$3LiAlH_4 + TiCl_3 \rightarrow 3LiCl + Ti + 3Al + 6H_2 \quad (1)$$

After ageing overnight, washing, and drying, the resulting black suspension was characterized. As shown by XRD, the diffraction pattern of the material mainly contained peaks with a weaker intensity related to the monoclinic phase of $LiAlH_4$ and additional peaks assigned to tetragonal TiH and residual $TiCl_3$ (Figure 4). No metallic Ti was observed and this was consistent with the ability of $LiAlH_4$ to reduce metal halides with the formation of their corresponding hydride [41]. Non-stoichiometric TiH_{2-x} has previously been reported to form when heating metallic Ti under hydrogen pressure at temperatures >300 °C [39,42]. However, under the current experimental conditions, it is possible that the hydrogen release upon reaction (1) directly interacts with the newly formed Ti nuclei to generate the corresponding hydride. The remaining $TiCl_3$ observed by XRD was unexpected owing to the large molar ratio (16:1) of $LiAlH_4$ compared to $TiCl_3$, and this indicated that the reduction of $TiCl_3$ by $LiAlH_4$ stopped during the process. This could be the result of the formation of a TiH layer at the surface of the $LiAlH_4$ nanoparticles significantly decreasing the contact area of $LiAlH_4$ and $TiCl_3$, and thus precluding any further reduction.

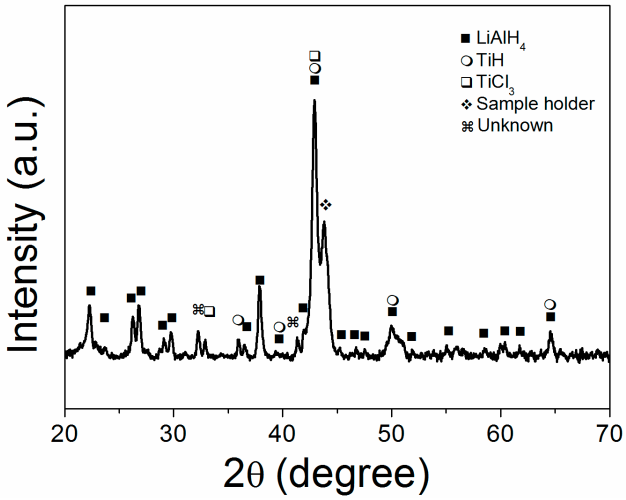

Figure 4. XRD of as-prepared Ti coated nanosized $LiAlH_4$.

Additional characterization by TEM revealed largely spherical particles with a broad particle size distribution ranging from 5 to 50 nm (Figure 5a,b,e). This corresponds to a significant increase in particle size as compared to the uncoated $LiAlH_4$ nanoparticles (Figure 2) and thus indicates the deposition of a TiH layer. Indeed, EDS analysis and elemental mapping revealed the Ti and Al content of the nanoparticles imaged and the even distribution of Ti on the $LiAlH_4$ nanoparticles (Figure 5c,d). Hence, it was believed that Ti was successfully deposited at the surface of the $LiAH_4$ nanoparticles. The weaker intensity of the XRD peaks related to $LiAlH_4$ in the Ti coated nanosized $LiAlH_4$ material also corroborates this conclusion (Figure 4), because upon coating the diffraction peak intensity of the core has been reported to significantly decrease [31].

Analysis of the hydrogen desorption properties of these Ti modified nanoparticles revealed a unique behavior (Figure 6). Nanosized $LiAlH_4$ modified with Ti almost fully decomposed through a single and extremely exothermic event recorded by DSC at 120 °C (Figure 6a,b). In comparison, bulk $LiAlH_4$ ball milled with $TiCl_3$ (material denoted bulk-$LiAlH_4$/Ti) decomposed following the known decomposition path of $LiAlH_4$—i.e., via Steps 1 and 2 (Figure 6c,d)—in agreement with previous reports [9,43,44]. This was confirmed by the XRD of bulk $LiAlH_4$/Ti after heating at 150, 200 and 300 °C.

As shown in Figure 6b, at 150 °C, bulk-$LiAlH_4$/Ti started partial decomposition to Li_3AlH_6 according to Step 1. Then at 180 °C, the $LiAlH_4$ phase totally converted to Li_3AlH_6 and at 300 °C, Li_3AlH_6 fully decomposed to LiH and Al following Step 2. In comparison, the diffraction pattern of nanosized $LiAlH_4$ coated with Ti heated at 150 °C after the single exothermic event showed that no

$LiAlH_4$ remained, while only a very small amount of Li_3AlH_6 was detected (Figure 7a). The remaining Li_3AlH_6 could be the result of unevenly or partially coated $LiAlH_4$ nanoparticles evolving to bulk size materials upon melting. However, this could not be confirmed since no apparent melting was detected by DSC peak (Figure 6a).

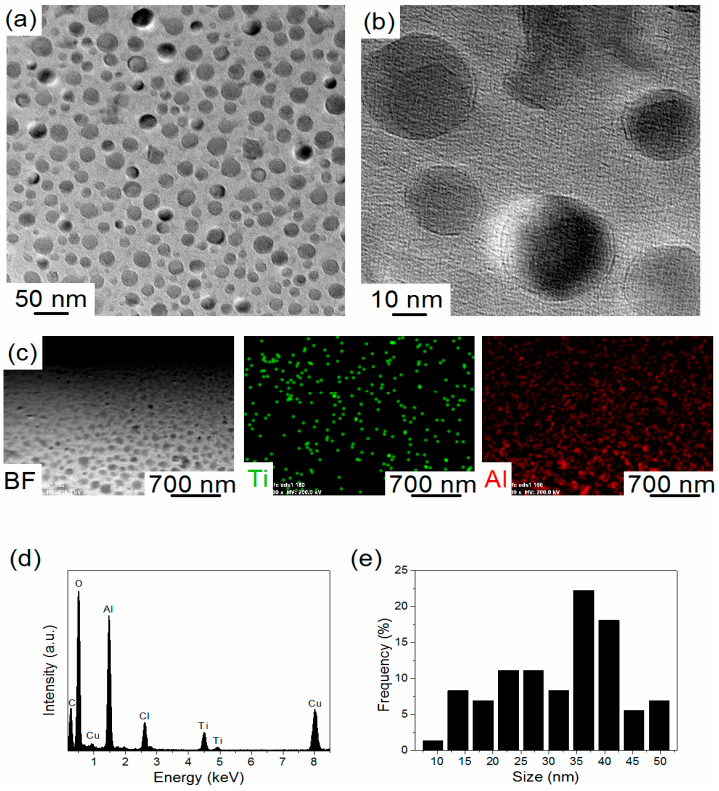

Figure 5. TEM images of (**a**,**b**) as-prepared Ti coated nanosized $LiAlH_4$ and corresponding (**c**) elemental mapping analysis; (**d**) EDS spectrum and (**e**) particle size distribution.

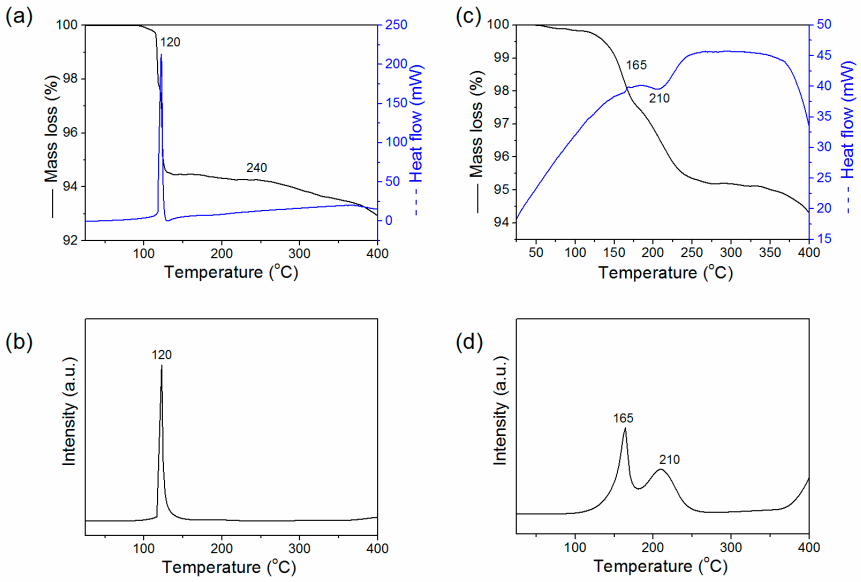

Figure 6. TGA/DSC for (**a**) as-prepared Ti coated nanosized $LiAlH_4$, (**c**) commercial bulk $LiAlH_4$ ball milled with $TiCl_3$, (**b**,**d**) respective hydrogen desorption profile as followed by mass spectrometry. No other gases than hydrogen were detected.

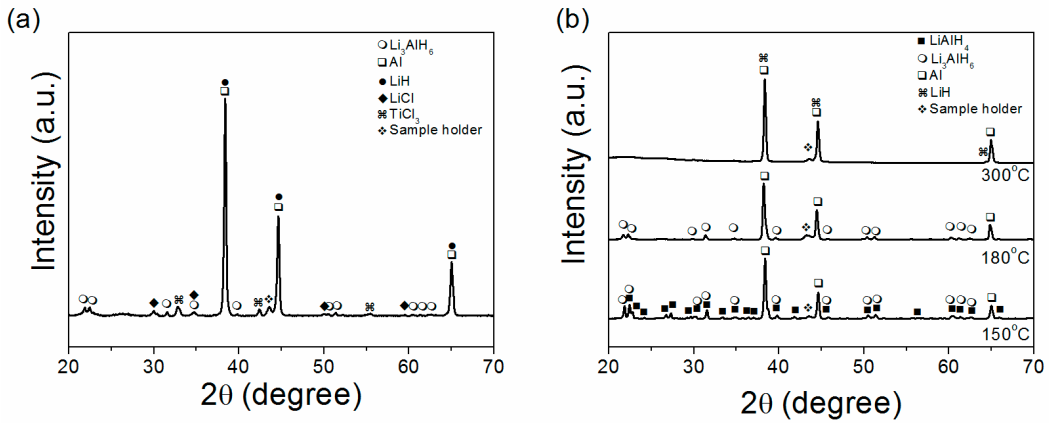

Figure 7. XRD of (**a**) as-prepared Ti coated nanosized $LiAlH_4$ after hydrogen release at 150 °C and (**b**) commercial bulk $LiAlH_4$ ball milled with $TiCl_3$ after thermal decomposition at 150, 180 and 300 °C.

Another possibility for the partial decomposition of Li_3AlH_6 is that the intended core–hell structure disintegrated under the sharp exothermic event as proven by TEM analysis of the dehydrogenated material (Figure 8), and consequently sprayed around undecomposed Li_3AlH_6. The observed suppression of melting as per bulk $LiAlH_4$ is also an indicator that $LiAlH_4$ was confined within a TiH shell.

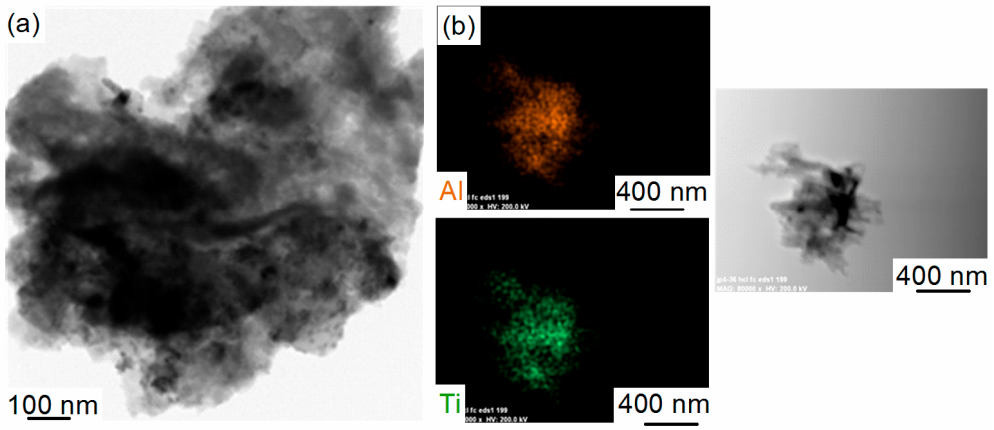

Figure 8. TEM images of (**a**) as-prepared Ti coated nanosized $LiAlH_4$ after hydrogen release at 150 °C and (**b**) corresponding elemental mapping analysis.

The possible core–shell structure disintegration could also be the reason of an appearance of LiCl and the disappearance of diffraction peaks related to TiH (Figure 7a). LiCl was not present in the as-prepared Ti coated nanosized $LiAlH_4$ (Figure 4), and this potentially indicates that more $LiAlH_4$ was exposed to react with $TiCl_3$ to form LiCl following reaction (1) during the exothermic event. The lack of TiH phase after the exothermic release of hydrogen also indicates a deterioration of the coating owing to the heat generated during the exothermic release of hydrogen. TiH has been reported to decompose at temperatures above 470 °C [45].

Furthermore, upon hydrogen release, nanosized $LiAlH_4$ coated with Ti lost about 5.7 mass % almost instantly near 120 °C. Taking into account the weight of $TiCl_3$ added to nanosized $LiAlH_4$, the theoretical hydrogen release for Step 1 should be reduced from 5.3 to 4.2 mass %, and from 2.6 to 2.1 mass % for both Steps 2 and 3. This corresponds to a theoretical hydrogen content of 6.3 mass % up to Step 2. The 5.7 mass % loss of the Ti coated nanosized $LiAlH_4$ thus corresponds to a close to full hydrogen release. Possible hydrogen release from TiH was unlikely to be noticeable in the hydrogen desorption profile. Assuming that nanoscale TiH was decomposed, this would correspond to an

additional amount of hydrogen of less than 0.1 mass %. Accordingly, this result implies a significant thermodynamic alternation induced by the synergetic effects of the Ti catalytic coating with $LiAlH_4$ nanosizing potentially involving the decompositions of both $LiAlH_4$ and Li_3AlH_6 in a rapid manner following the direct reaction (2).

$$2LiAlH_4 \rightarrow 2LiH + 2Al + 3H_2 \quad (2)$$

Although, the currently modified properties of Ti modified nanosized $LiAHl_4$ are unsuitable for hydrogen storage purposes, this finding implies that the strategy of catalytic coating on hydride nanoparticles offers a more versatile avenue to modifying the hydrogen storage properties of a hydride to a larger extent when compared to mechanically activated $LiAlH_4$ with Ti.

3. Materials and Methods

All experiments were performed under an inert atmosphere in an argon filled glove box (O_2 and H_2O < 1 ppm) from LC Technology (Salisbury, MD, USA) $LiAlH_4$ 2.0 M in THF, titanium (III) chloride, 1-dodecanethiol, and anhydrous pentane were purchased from Sigma Aldrich (Sydney, Australia) and used as received. Lithium aluminum hydride ($LiAlH_4$, 95%) was purchased from Sigma Aldrich (Sydney, Australia), and purified by dissolving it in a large amount of diethyl ether and recrystallizing it from the filtrate solution.

3.1. Synthesis of $LiAlH_4$ Nanoparticles

In a typical synthesis, 5 mL of a commercial $LiAlH_4$ solution (2.0 M in THF) was placed in a vial and stirred gently with 10 μL (2 mg) of 1-dodecanethiol. The vial was then closed tightly and the solution was left to age overnight. The solvent was then evaporated under a moderate vacuum until a viscous paste was formed. The later was fully dried at 30 °C under dynamic vacuum. The yield was around 410 mg, which is slightly higher than the 382 mg theoretical yield owing to remaining THF bonded to $LiAlH_4$.

3.2. Coating of the $LiAlH_4$ Nanoparticles with Ti

The as-synthesized $LiAlH_4$ nanoparticles (100 mg) were suspended in 20 mL of pentane, under magnetic stirring at 600 rpm to form a milky suspension. 25 mg of $TiCl_3$ ($8.1\ 10^{-3}$ mol·L^{-1}) was then suspended in a 10 mL solution of pentane and then added dropwise to the suspension of the $LiAlH_4$ nanoparticles at a rate of 50 μL·min^{-1}. After a few minutes, the suspension turned black and was allowed to age overnight before separation by centrifugation and drying under dynamic vacuum overnight.

3.3. Preparation of Reference Material Ball Milled $LiAlH_4$ with $TiCl_3$

As a reference, commercial bulk $LiAlH_4$ was ball milled with $TiCl_3$ (5 mol %) using a Retsch Mixer Mill MM 400 (Haan, Germany). The mixture was milled for 10 min at 20 Hz three times with a ball to powder weight ratio of 135:1.

3.4. Characterization

Transmission Electron Microscopy (TEM) and Energy Dispersive X-ray Spectroscopy (EDS) were performed with a Philips CM200 (Sydney, Australia) operated at 200 kV. The materials were dispersed in pentane, dropped onto a carbon coated copper grid, and dried in an argon filled glovebox before transfer to the microscope in a quick manner as to minimize air exposure. X-ray Diffraction (XRD) was performed by using a PANalytical X'pert Multipurpose XRD system (Sydney, Australia) operated at 40 mA and 45 kV with a monochromated Cu Kα radiation (λ = 1.541 Å); step size = 0.01, 0.02 or 0.05; time per step = 10 or 20 s/step. The materials were protected against oxidation from air by a Kapton foil covering a stainless steel sample holder. Hydrogen desorption profiles were acquired

by Thermogravimetric Analysis (TGA)/Differential Scanning Calorimetry (DSC) coupled with Mass Spectrometry (MS) using a Mettler Toledo TGA/DSC (Sydney, Australia) 1 coupled with an Omnistar MS. Measurements were conducted with alumina crucibles at 10 °C·min^{-1} under an argon flow of 25 mL·min^{-1}. Masses between m/z = 2 and 100 were recorded. Reversibility was checked by manually performing hydrogen absorption/desorption cycles with a homemade Sievert apparatus and a stainless steel sample holder operated at 300 °C, with 7 MPa hydrogen pressure for absorption and 0.01 MPa for desorption. No significant reversibility was observed.

4. Conclusions

An effective downsizing and coating approach was developed and demonstrated that it is possible to synthesize isolated $LiAlH_4$ nanoparticles to a certain extent and ultimately modify the hydrogen storage properties of $LiAlH_4$. Once coated with Ti, nanosized $LiAlH_4$ was found to decompose at 120 °C in a single exothermic event with a 5.7 mass % and instant hydrogen release. This finding implies a significant thermodynamic alternation induced by the synergetic effects of the Ti catalytic coating with $LiAlH_4$ nanosizing that ultimately changed its decomposition path to $LiAlH_4 \rightarrow Al + LiH + 3/2H_2$. This finding also demonstrates that the hydrogen storage properties of $LiAlH_4$ should be size dependent and thus provides a new avenue to modify the properties of $LiAlH_4$ through particle size effects. Due to the violent exothermic nature of its decomposition, this material is considered not viable for practical hydrogen storage purposes. However, Ti coated nanosized $LiAlH_4$ offers a unique alternative as compared to hydrides which only supply hydrogen via an endothermic reaction. It enables applications where larger amounts of hydrogen and heat are both needed at the same time and rapidly, e.g., for compact explosives and fire starters.

Acknowledgments: Financial support by UNSW Internal Research Grant program is gratefully acknowledged. We appreciate the use of instruments in the Mark Wainwright Analytical Centre at UNSW.

Author Contributions: Lei Wang carried out all the experimental work which was conceived and designed with Kondo-Francois Aguey-Zinsou.

Conflicts of Interest: The authors declare no conflict of interest.

References

1. Dornheim, M. *Thermodynamics of Metal Hydrides: Tailoring Reaction Enthalpies of Hydrogen Storage Materials*; In Tech: Rijeka, Croatia, 2011.
2. Jang, J.W.; Shim, J.H.; Cho, Y.W.; Lee, B.J. Thermodynamic calculation of $LiH \leftrightarrow Li_3AlH_6 \leftrightarrow LiAlH_4$ reactions. *J. Alloys Compd.* **2006**, *420*, 286–290. [CrossRef]
3. Varin, R.A.; Czujko, T.; Wronski, Z.S. *Nanomaterials for Solid State Hydrogen Storage*; Springer: Berlin, Germany, 2009.
4. Lai, Q.; Paskevicius, M.; Sheppard, D.A.; Buckley, C.E.; Thornton, A.W.; Hill, M.R.; Gu, Q.; Mao, J.; Huang, Z.; Liu, H.K.; et al. Hydrogen storage materials for mobile and stationary applications: Current state of the art. *ChemSusChem* **2015**, *8*, 2789–2825. [CrossRef] [PubMed]
5. Lacina, D.; Yang, L.; Chopra, I.; Muckerman, J.; Chabal, Y.; Graetz, J. Investigation of $LiAlH_4$–THF formation by direct hydrogenation of catalyzed Al and LiH. *Phys. Chem. Chem. Phys.* **2012**, *14*, 6569–6576. [CrossRef] [PubMed]
6. Orimo, S.I.; Nakamori, Y.; Eliseo, J.R.; Züttel, A.; Jensen, C.M. Complex hydrides for hydrogen storage. *Chem. Rev.* **2007**, *107*, 4111–4132. [CrossRef] [PubMed]
7. Varin, R.A.; Zbroniec, L. The effects of nanometric nickel (n-Ni) catalyst on the dehydrogenation and rehydrogenation behavior of ball milled lithium alanate ($LiAlH_4$). *J. Alloy. Compd.* **2010**, *506*, 928–939. [CrossRef]
8. Li, Z.; Zhai, F.; Wan, Q.; Liu, Z.; Shan, J.; Li, P.; Volinsky, A.A.; Qu, X. Enhanced hydrogen storage properties of $LiAlH_4$ catalyzed by $CoFe_2O_4$ nanoparticles. *RSC Adv.* **2014**, *4*, 18989–18997. [CrossRef]
9. Amama, P.B.; Grant, J.T.; Shamberger, P.J.; Voevodin, A.A.; Fisher, T.S. Improved Dehydrogenation Properties of Ti-Doped $LiAlH_4$: Role of Ti Precursors. *J. Phys. Chem.* **2012**, *116*, 21886–21894. [CrossRef]

10. Easton, D.S.; Schneibel, J.H.; Speakman, S.A. Factors affecting hydrogen release from lithium alanate ($LiAlH_4$). *J. Alloy Compd.* **2005**, *398*, 245–248. [CrossRef]
11. Fu, J.; Tegel, M.; Kieback, B.; Röntzsch, L. Dehydrogenation properties of doped $LiAlH_4$ compacts for hydrogen generator applications. *Int. J. Hydrog. Energy* **2014**, *39*, 16362–16371. [CrossRef]
12. Liu, X.; McGrady, G.S.; Langmi, H.W.; Jensen, C.M. Facile cycling of Ti-doped $LiAlH_4$ for high performance hydrogen storage. *J. Am. Chem. Soc.* **2009**, *131*, 5032–5033. [CrossRef] [PubMed]
13. Graetz, J.; Wegrzyn, J.; Reilly, J.J. Regeneration of lithium aluminum hydride. *Chem. Inf.* **2008**, *130*, 17790–17794. [CrossRef] [PubMed]
14. Ashby, E.C.; Brendel, G.J.; Redman, H.E. Direct Synthesis of Complex Metal Hydrides. *Inorg. Chem.* **1963**, *2*, 499–504. [CrossRef]
15. Wang, J.; Ebner, A.D.; Ritter, J.A. Physiochemical Pathway for Cyclic Dehydrogenation and Rehydrogenation of $LiAlH_4$. *J. Am. Chem. Soc.* **2006**, *128*, 5949–5954. [CrossRef] [PubMed]
16. Wang, J.; Ebner, A.D.; Ritter, J.A. Synthesis of metal complex hydrides for hydrogen storage. *J. Phys. Chem.* **2007**, *111*, 14917–14924. [CrossRef]
17. Chen, J.; Kuriyama, N.; Xu, Q.; Takeshita, H.T.; Sakai, T. Reversible hydrogen storage via titanium-catalyzed $LiAlH_4$ and Li_3AlH_6. *J. Phys. Chem.* **2001**, *105*, 11214–11220. [CrossRef]
18. Wang, L.; Rawal, A.; Quadir, M.Z.; Aguey-Zinsou, K.F. Nanoconfined lithium aluminium hydride ($LiAlH_4$) and hydrogen reversibility. *Int. J Hydrog. Energy* **2017**, *42*, 14144–14153. [CrossRef]
19. Wang, L.; Quadir, M.Z.; Aguey-Zinsou, K.F. Ni coated LiH nanoparticles for reversible hydrogen storage. *Int. J Hydrog. Energy* **2016**, *41*, 6376–6386. [CrossRef]
20. Christian, M.L.; Aguey-Zinsou, K.F. Core–shell strategy leading to high reversible hydrogen storage capacity for $NaBH_4$. *ACS Nano* **2012**, *6*, 7739–7751. [CrossRef] [PubMed]
21. Bogdanović, B.; Schwickardi, M. Ti-doped $NaAlH_4$ as a hydrogen-storage material—Preparation by Ti-catalyzed hydrogenation of aluminum powder in conjunction with sodium hydride. *Appl. Phys.* **2001**, *72*, 221–223. [CrossRef]
22. Blanchard, D.; Brinks, H.W.; Hauback, B.C.; Norby, P. Desorption of $LiAlH_4$ with Ti- and V-based additives. *Mat. Sci. Eng. Solid* **2004**, *108*, 54–59. [CrossRef]
23. Kojima, Y.; Kawai, Y.; Haga, T.; Matsumoto, M.; Koiwai, A. Direct formation of $LiAlH_4$ by a mechanochemical reaction. *J. Alloy. Compd.* **2007**, *441*, 189–191. [CrossRef]
24. Liu, X.; Langmi, H.W.; Beattie, S.D.; Azenwi, F.F.; McGrady, G.S.; Jensen, C.M. High-yield direct synthesis of $LiAlH_4$ from LiH and Al in the Presence of $TiCl_3$ and Me_2O. *J. Am. Chem. Soc.* **2011**. [CrossRef]
25. Zhou, C.; Fang, Z.Z.; Ren, C.; Li, J.; Lu, J. Effect of Ti intermetallic catalysts on hydrogen storage properties of magnesium hydride. *J. Phys. Chem.* **2013**, *117*, 12973–12980. [CrossRef]
26. Walker, G. *Solid-State Hydrogen Storage: Materials and Chemistry*; Elsevier: Amsterdam, The Netherlands, 2008.
27. Kojima, Y.; Kawai, Y.; Matsumoto, M.; Haga, T. Hydrogen release of catalyzed lithium aluminum hydride by a mechanochemical reaction. *J. Alloy Compd.* **2008**, *462*, 275–278. [CrossRef]
28. Sun, Y.; Shen, C.; Lai, Q.; Liu, W.; Wang, D.W.; Aguey-Zinsou, K.F. Tailoring magnesium based materials for hydrogen storage through synthesis: Current state of the art. *Energy Storage Mater.* **2017**. [CrossRef]
29. De Jongh, P.E.; Adelhelm, P. Nanosizing and nanoconfinement: New strategies towards meeting hydrogen storage goals. *ChemSusChem* **2010**, *3*, 1332–1348. [CrossRef] [PubMed]
30. Wan, X.; Shaw, L.L. Novel dehydrogenation properties derived from nanoscale $LiBH_4$. *Acta Mater.* **2011**, *59*, 4606–4615. [CrossRef]
31. Ghosh Chaudhuri, R.; Paria, S. Core/shell nanoparticles: Classes, properties, synthesis mechanisms, characterization, and applications. *Chem. Rev.* **2011**, *112*, 2373–2433. [CrossRef] [PubMed]
32. Cushing, B.L.; Kolesnichenko, V.L.; O'Connor, C.J. Recent advances in the liquid-phase syntheses of inorganic nanoparticles. *Chem. Rev.* **2004**, *104*, 3893–3946. [CrossRef] [PubMed]
33. Bensebaa, F. Chapter 2—Wet production methods. In *Interface Science and Technology*; Farid, B., Ed.; Elsevier: Amsterdam, The Netherlands, 2013; pp. 85–146.
34. Wang, L.S.; Hong, R.Y. Synthesis, surface modification and characterisation of nanoparticles. *Adv. Nanocompos.* **2011**, *18*, 7533–7548.
35. Kühnle, A.; Vollmer, S.; Linderoth, T.R.; Witte, G.; Besenbacher, F. Adsorption of dodecanethiol on Cu (110): Structural ordering upon thiolate formation. *Langmuir* **2002**, *18*, 5558–5565. [CrossRef]

36. Stein, S.E. *"Mass Spectra" in NIST Chemistry WebBook. In NIST Standard Reference Database Number 69*; NIST Mass Spec Data Center: Gaithersburg, MD, USA, 2016.
37. Chaudhuri, S.; Muckerman, J.T. First-principles study of Ti-catalyzed hydrogen chemisorption on an al surface: A critical first step for reversible hydrogen storage in $NaAlH_4$. *J. Phys. Chem.* **2005**, *109*, 6952–6957. [CrossRef] [PubMed]
38. Wipf, H.; Kappesser, B.; Werner, R. Hydrogen diffusion in titanium and zirconium hydrides. *J. Alloy Compd.* **2000**, *310*, 190–195. [CrossRef]
39. Livanov, V.A.; Bukhanova, A.A.; Kolachev, B. *Hydrogen in Titanium*; Israel Program for Scientific Translations: Jerusalem, Israel, 1965.
40. Gu, J.; Zhang, Y.-W.; Tao, F. Shape control of bimetallic nanocatalysts through well-designed colloidal chemistry approaches. *Chem. Soc. Rev.* **2012**, *41*, 8050–8065. [CrossRef] [PubMed]
41. Patnaik, P. *Handbook of Inorganic Chemicals*; McGraw-Hill: New York, NY, USA, 2003.
42. Rittmeyer, P.; Wietelmann, U. *Hydrides. Ullmann's Encyclopedia of Industrial Chemistry*; Wiley-VCH Verlag GmbH & Co: Berlin, Germany, 2000.
43. Liu, X.; Beattie, S.D.; Langmi, H.W.; McGrady, G.S.; Jensen, C.M. Ti-doped $LiAlH_4$ for hydrogen storage: Rehydrogenation process, reaction conditions and microstructure evolution during cycling. *Int. J. Hydrog. Energy* **2012**, *37*, 10215–10221. [CrossRef]
44. Resan, M.; Hampton, M.D.; Lomness, J.K.; Slattery, D.K. Effects of various catalysts on hydrogen release and uptake characteristics of LiAlH. *Int. J. Hydrog. Energy* **2005**, *30*, 1413–1416. [CrossRef]
45. Bhosle, V.; Baburaj, E.G.; Miranova, M.; Salama, K. Dehydrogenation of TiH2. *Mat. Sci. Eng. A Struct.* **2003**, *356*, 190–199. [CrossRef]